International Journal of Nanomedicine

Dovepress
open access to scientific and medical research

Open Access Full Text Article

ORIGINAL RESEARCH

Delivery luteolin with folacin-modified nanoparticle for glioma therapy

This article was published in the following Dove Press journal:
International Journal of Nanomedicine

Cong Wu
Qian Xu
Xinyue Chen
Jiagang Liu

Department of Neurosurgery, West China Hospital, West China Medical School, Sichuan University, Chengdu 610041, People's Republic of China

Background: Glioblastoma mutliforme is the most common and has the poorest prognosis of any malignant tumor of the central nervous system. Luteolin, the most abundant xanthone extracted from vegetables and medicinal plants, has been shown to have treatment effects in various cancer cell types. Luteolin is however, hydrophobic and has poor biocompatibility, which leads to low bioavailability.

Patients and methods: In this study, folic acid modifiedpoly(ethylene glycol)-poly(e-caprolactone) (Fa-PEG-PCL) nano-micelles was used to encapsulate the luteolin, creating luteolin loaded PEG-PCL (Lut/Fa-PEG-PCL) micelles to treat glioma both in vitro and in vivo.

Results: When compared with the free luteolin and Lut/MPEG-PCL, Lut/Fa-PEG-PCL induced a significant cell growth inhibition and more apoptosis of GL261 cells both in vitro and in vivo. The safety assessment also showed no obvious side effects were observed in mice which were administrated with free luteolin or Lut/MPEG-PCL and Lut/Fa-PEG-PCL.

Conclusion: These results suggested Lut/Fa-PEG-PCL may be used as an excellent intravenously injectable formulation for the treatment and chemoprevention.

Keywords: luteolin, PEG-PCL, glioma, folic acid, apoptosis

Introduction

Glioblastoma mutliforme (GBM) is the most common and has the poorest prognosis of any malignant tumor of the central nervous system, which is classified as the fourth stage by WHO.[1–4] It turns out that the morbidity of GBM among people is as high as 3.19/100,000 through age adjustment by Central Brain Tumor Registry of the United States (CBTRUS). GBM accounts for 45.2% of all primary central nervous system malignant neoplasms and a high 54% of glioma's.[5] Its morbidity rises as age grows, comes to the peak between 75 and 84 years old, then declines after 85 years old. Besides, the average age of primary-care patients is 64 years old. As GBM is characterized biologically by diffuse growth, strong invasion and easy relapse, we conform to the rules as follows: safe resection of tumor to maximum range, individualized fractional radiotherapy and chemotherapy associated with new systemic chemotherapy. The median survival time for GBM patients remains 14 to 15 months only. Therefore, seeking for a effective drug has become a hot spot now in antiglioma research.

Luteolin has a typical C6-C3-C6 structure, which is strongly associated with its biochemical function and biological activity. Luteolin is widely distributed in vegetables and medicinal plants like carrot, cabbage, thyme and schizonepeta, whereas luteolin is widely distributed in the form of glycoside in celery, green

Correspondence: Jiagang Liu
Department of Neurosurgery, West China Hospital, West China Medical School, Sichuan University, Chengdu 610041, People's Republic of China
Tel +86 288 542 2136
Fax +86 288 550 2796
Email jiagang_liu@163.com

submit your manuscript | www.dovepress.com
DovePress
http://doi.org/10.2147/IJN.S214585

capsicum and perilla leaves.[6,7] Clinical epidemiology study demonstrates that luteolin has various biological and pharmacological activities, such as antibacterial action, antiviral action, antioxidation activity, antitumor activity, hypoglycemic effect, hypolipidemic effect, hypotensive effect and immunomodulatory functions, etc.[8–10] In recent years, numerous researchers have found that luteolin has broad-spectrum antitumor activities with many different forms. By regulating intricate signal transduction pathways, luteolin presents multiple antineoplastic effects, such as antitumor cell proliferation, anticarcinogen effects, blocking cell cycle progression, inducing tumor cells apoptosis,inhibiting the infiltration and metastasis of tumor and the growth of new vessels, etc.[11–15]

It is rather difficult for luteolin to reach the target region of glioma because luteolin is sparingly soluble in water and thus its bioavailability is fairly low orally, and it is usually very difficult to go through blood-brain barrier (BBB) or blood tumor barrier (BTB). Even though luteolin penetrates BBB and reaches the target region of glioma, it is hard to attain sustaining, effective drug concentration to inhibit or kill tumor cells. Hopefully, nanoparticle by intracephalic administration may be a method to resolve the problem.[16–20] It is a new idea for GBM treatment in future to lucubrate new intracephalic delivery carriers including nanoparticle and utilize their unique surface properties, good biocompatibility and biodegradation. In that way, we can achieve the goals to carry antitumor medicine through BBB or BTB to reach the target region of neoplasm and release drug continuously, eventually attaining drug concentration needed to inhibit or kill tumor cells and reducing the drug's toxicity to normal cells.

Folate receptor is a kind of glycoprotein anchored to membrane through phosphatidylinositol glycan.[21–23] A study has found that folate receptor presents increased expression and activity in many tumor tissues compared with that in normal tissues, which is strongly correlated with clinical stages of tumor. Normal tissues and cells rarely express folate receptor except the expression of placenta, choroid and the low expression of pulmo, thyroid, kidney. Folate receptor has become a target spot for the treatment of broad-spectrum malignancy. Meanwhile, folic acid, as a natural ligand for folate receptor, is characterized by havingno antigenicity, a low relative molecular weight, no immunogenicity, is inexpensive and easy to obtain, has a high stability, is easy to bond with other substance chemically and maintains the binding activity with folate receptor, etc. Monomethoxy poly (ethylene glycol)-poly(ε-caprolactone) (MPEG-PCL) which is a kind of polymeride constituted by monomethoxy polyethylene glycol (MPEG) and poly-ε-caprolactone (PCL), widely used nanoparticles now, is characterized by good biocompatibility and biodegradation, is easy to pass through BBB or BTB and has high drug-loading efficiency and so forth, is regarded as relatively ideal drug-loading particles for antitumor research of central nervous system so far.

By modifying MPEG-PCL with folic acid and constructing luteolin/Fa-PEG-PCL nanoparticles, our research takes the combined methods, studying both in vivo and vitro, to focus on the antitumor effect of luteolin in varied key links such as antitumor cell proliferation, inducing tumor cell apoptosis and inhibiting the infiltration and metastasis of tumor, and so forth, to study the specific antiglioma effect of luteolin and its relative pathways. We also compare the difference between free luteolin and luteolin/Fa-PEG-PCL nanoparticles in antiglioma action, explore and demonstrate the possible mechanism of the action and hope to provide a new idea for GBM treatment.

Materials and methods

Materials

Materials were purchased from standard sources: luteolin from Sigma (St Louis, MO, USA); MTT from Sigma; DMEM and FBS from Gibco BRL (Waltham, MA, USA); methanol and acetic acid (HPLC grade) from Fisher Scientific (Waltham, MA, USA); and dimethyl sulfoxide (DMSO) and acetone from KeLong Chemicals (Chengdu, China). Antibodies used include rat anti-mouse CD31 polyclonal antibody (BD Pharmingen™, Franklin Lake, NJ, USA), rabbit anti-mouse PCNA antibody (Abcam, Cambridge, UK), and rhodamine-conjugated secondary antibody (Abcam). NH2-PEG-PCL was purchased from ruixi Biological Technology Company (Xian, China).

C57 mice (6–8 weeks) and Sprague Dawley (SD) rats were purchased from the Animal Center Laboratory of Beijing HFK Bioscience Co Ltd (Beijing, People's Republic of China). All mice were housed in a controlled temperature of 20–22°C, with a relative humidity of 50–60% and 12 hr light-dark cycles. The animals were provided with standard laboratory chow and tap water ad libitum. All animal procedures were performed following the protocol approved by the Institutional Animal Care and Treatment Committee of Sichuan University (Chengdu, People's Republic of China) and treated humanely throughout the experimental period.

Molecular dynamic simulation

Luteolin was built at first with Marvin Sketch (http://www.chemaxon.com) and optimized at the molecular mechanical level with the MMFF94 method.[24] Then, it was further optimized at the semiempirical level using the AM1 method with the Fletcher–Reeves algorithm by employing Hyperchem software (HyperChem, Professional 8.0, Hypercube, Inc., Gainesville, Florida, USA). The structures of FA-PEG-PCL and luteolin were constructed, optimized and simulated according to a strategy described in a published document.[24]

To understand in detail the mechanism by which luteolin passively targets tumor tissue, interactions between the biblock copolymer Fa-PEG-PCL and luteolin in different circumstances were investigated with molecular dynamic simulation. Luteolin was docked randomly to the simulated biblock copolymer Fa-PEG-PCL at first by merging it to the Fa-PEG-PCL in the workspace of HyperChem to obtain the initial structure of complex composed of luteolin and Fa-PEG-PCL. Then, two stages of Langevin dynamic simulations were performed in an effort to explore interactions between the two components of the complex in water. In the process of simulation, the temperature, friction coefficient and random seed were set to 300 K, 0.05 ps-1 and 0, respectively. CHARMM27 was chosen as the force field. At the first stage of simulation, interactions in water were simulated and the solvation effect was considered implicitly by setting the scale factor for the dielectric permittivity to 80. At each stage, the run time was set to 500 ps.

Synthesis of MPEG-PCL diblock copolymer and Fa-PEG-PCL

The MPEG with a molecular weight of 2000D was dried and placed in a flask, after magnetic stirring at a constant temperature of 105°C for 90 mins under a vacuum condition.

The preprocessed MPEG and ε-caprola were simultaneously put in a dry glass ampoule filled with nitrogen; then, ($Sn(Oct)_2$) was added, stirred and mixed and reacted at 130°C for 6 hrs. MPEG will open the cyclic structure of ε-caprolactone to form MPEG-PCL diblock polymer, in which both MPEG and PCL have a molecular weight of 2000D. The purified MPEG-PCL copolymer was placed in a desiccator to be reserved.

First, folic acid (100 mg) and NH_2-PEG-PCL (200 mg) were dissolved in 4 mL of dimethylsulfoxide (DMSO), respectively. Then, the solutions were introduced to a flask, and DMAP (150 mg) and DCC (130 mg) were added as catalyst. After stirring at room temperature under nitrogen for 10 hrs, the resulting solution was dialyzed (MWCO =1000 Da) against water. The purified Fa-PEG-PCL was freeze-dried and stored at 4°C before further use. ^{1}H nuclear magnetic resonance spectroscopy (^{1}H-NMR, Bruker Avance III 400, Bruker, Germany) and Fourier transform infrared spectroscopy (FTIR, Nicolet 200 SXV, Thermo Fisher Scientific, Waltham, MA, USA) were performed to study the chemical structure of the obtained polymers. UV-vis absorption spectroscopy of the samples was recorded using a spectrophotometer (UV-2600, SHIMADZU, Japan).

Preparation of luteolin/MPEG-PCL nanoparticles modified by folic acid

Modified luteolin/MPEG-PCL particles were synthesized by self-assembly method using the unique self-assembly characteristic of MPEG-PCL diblock copolymers. 5 mg of luteolin, 85 mg of MPEG-PCL diblock copolymer and 10 mg of folic acid-modified PEG-PCL were dissolved in acetone, and the above liquid was evaporated under reduced pressure in a 55°C water bath to remove the acetone, then a film is formed and finally deionized water is added to the film for hydration, and the folic acid-modified luteolin/MPEG-PCL fine particle solution is completely obtained by hydration. It was lyophilized at 4°C and stored for reserving. The folate-modified MPEG-PCL was replaced with unmodified MPEG-PCL, and the prepared solution was luteolin/MPEG-PCL nanoparticle solution.

Luteolin/Fa-PEG-PCL particle characteristic detection

Drug loading and packaging rate determination

10 mg of lycopene-preserved luteolin/Fa-PEG-PCL microparticles was dissolved in 0.1 mL of methanol to calculate the concentration of luteolin. The content of luteolin in the microparticles was determined by high-performance liquid-phase chromatography (Japanese Shimadzu LC-20AD), and the drug loading (DL) and encapsulation rate (ER) of luteolin/Fa-PEG-PCL microparticles were, respectively, calculated by formula (1) and formula (2).

$$DL = Drug/(Ploymer + Drug) \times 100\% \quad (1)$$

$$ER = experimental\ drug\ loading/Theoretical\ drug\ loading \times 100\% \quad (2)$$

Physical and chemical property determination

Nanoparticle size analyzer: The solution containing the luteolin/Fa-PEG-PCL microparticle sample was diluted with distilled water, and the size and zeta potential of the luteolin/Fa-PEG-PCL microparticles were measured by a dynamic light scattering principle using a nanoparticle size analyzer (British Malvern Nano-ZS 90) at 25°C. The operation was repeated for three times.

Transmission electron microscopy: diluting the diluted luteolin/Fa-PEG-PCL particle suspension onto the copper grid of the transmission electron microscope; then, the background was stained with a weight-to-volume ratio of 2% phosphotungstate solution for 10 mins. After drying, the morphological characteristics of luteolin/Fa-PEG-PCL particles were observed by transmission electron microscopy, and 30 particles were selected to measure their diameters. The average diameter of the particles.

In vitro release assay

1 mL of free luteolin in DMSO, 1 mL of luteolin/MPEG-PCL microparticles and 1 mL luteolin/Fa-PEG-PCL solution were added to the dialysis bag (American Sigma, St. Louis, MO, USA) and placed in 20 mL of phosphate buffer containing 0.5% Tween-80, stirring carefully and incubating at 37°C. At different time points, 200 μL samples were taken from the outside of the dialysis bag, and an equal amount of fresh buffer was added after sampling. The content of luteolin in the sampled samples was determined by HPLC (Japanese Shimadzu LC-20AD). The operation was repeated for three times.

Pharmacokinetic study

Male SD rats (weight 200 g±20 g) were randomly divided into three groups, 5 in each group. Rats in three groups were anesthetized with chloral hydrate, rats were given intravenous injection, one group was given free luteolin (luteolin: 50 mg/kg), the second group was given luteolin/MPEG-PCL particles (luteolin: 50 mg/kg), and the third group was given luteolin/Fa-PEG-PCL microparticles (luteolin: 50 mg/kg); blood samples were collected from the carotid artery at the preset time points (pre-dose, 15 min, 30 min, 1 h, 2 h, 4 h, 8 h, 12 h and 24 h). Plasma was separated and Lu was extracted from plasma with acetonitrile; supernatant fluid was collected and evaporated to dryness by nitrogen blowing. The dry residues were dissolved in methanol for HPLC analysis. The content of luteolin in the serum was determined by HPLC (Japanese Shimadzu LC-20AD), and related indicators of pharmacokinetics were calculated by using DAS software (DAS version 2.1.1,Chinese Mathematical Pharmacology Committee).

Cell culture

GL261 cells were obtained from American Type Culture Collection (ATCC). GL261 cells were cultured in DMEM medium supplement with 10% FBS and maintained in 37° C humidified incubator with 5% CO_2 atmosphere.

MTT assay for cell viability

GL261 cells were seeded in 96-well plates at a cell density of 3×10^3 tumor cells per cell culture well, cell culture medium at 100 μl/well, cultured at 37°C, 5% carbon dioxide overnight. The next day, different concentrations of drugs were added to the cell culture medium (from 0.4 μg/mL to 25 μg/mL). Twenty μl of MTT solution with a concentration of 5mg/ml were added to each cell culture well and incubated for 3 h after the adding drug for 24 h and 48 h. Then, the cell culture solution was poured out, 150 μL DMSO was added to each cell well, and shaken on a shaker for 10 mins; the absorbance was measured at a wavelength of 570 nm using a microplate reader.

Flow cytometry for apoptosis

When the cells were grown to 90% full, GL261 cells were seeded in 6-well plates at a cell density of 2×10^5 cells per well. The cell culture medium was 2 mL per well and cultured overnight. The next day, the double medium was aspirated, and then the medium containing different concentrations of the drug was added. After treatment for 24 hrs, the cells were digested with trypsin and collected, washed twice with sterile PBS, and then stained with apoptosis kit, incubated for 20 mins at room temperature. At last, apoptosis was detected on the machine.

Establishment of subcutaneous model of glioma

The GL261 cells were cultured at 37°C, 5% carbon dioxide culture conditions, until the cells were over 90%. The cells were collected. Finally, the cell concentration was adjusted to 1×10^7 per mL with DMEM medium, ready for inoculation. 100 μl cell solution was injected subcutaneously in the right front abdomen of C_{57} mice.

Establishment of an intracranial model of glioma

The GL261 cells were cultured at 37°C, 5% carbon dioxide culture conditions, until the cells were over 90%. The cells were collected. Finally, the cell concentration was adjusted to 2×10^7 per ml with DMEM medium, ready for inoculation and inoculated in intratumoral of C57 mice, 5 μL per mouse.

Anti tumor research

Based on the glioma model above, the tumor volume begins to be grouped up to about 100 mm^3 (the volume calculation formula is $V=0.52\times a\times b^2$, where a is the length and b is the width). The nude mice were divided into five groups of normal saline group (NS), blank microparticle group (EM), free luteolin drug group (F-Lut), luteolin nanodrug group (Lut-M), and folic acid-modified luteolin nanometer (Fa-Lut). There were seven mice in each group. The dose is 50 mg/kg, once every days, and the tumor volume is measured every two days. In the intracranial tumor model, the third day of administration was administered, and when the cachexia of the mouse appeared, the tumor size was observed by living body imaging.

TUNEL assay

The paraffin-embedded tumor tissue was cut into 5 μm sections and went through deparaffinage procedure. After fixation with 4% paraformaldehyde solution for 15 mins, 100 μL of proteinase K solution at a concentration of 20 μg/mL was added and incubated at room temperature for 8 mins. Then, tumor sections were washed twice with PBS solution and fixed again with 4% paraformaldehyde for 5 mins. 100 μL of equilibration buffer was added for 10 mins, followed by 50 μL TdT reaction mixture dropped to the tissue section, and then incubated at 37°C in the dark for 1 hr. Finally, the sections were immersed in 2× SSC reaction stop solution for 15 mins and washed with PBS. The stained sections were sealed and observed under a fluorescence microscope (Olympus, Japan).

Immunohistochemical detection of tumor proliferation activity

The fresh tumor tissue was sectioned with a cryostat, the tissue thickness was 5 μm, and the tissue sections were adhered to the slide glass and were washed with pre-cooled PBS for twice. The tumor sections were fixed with precooled acetone, fixed at 4°C for 20–30 mins and washed with PBS for 3 times. Each tumor tissue was blocked with goat serum for 30 mins. And tumor tissue was stained and incubated with PCNA antibody (1:100) overnight at 4°C in a wet box. Following wash with PBS, goat anti-rabbit horseradish peroxidase (HRP)-labeled secondary antibody was added and incubated at 37°C for 1 hr. Then, diaminobenzidine (DAB) solution was added for color rendering and hematoxylin was used for nuclei staining in each tissue section. The stained sections were observed under a light microscope (Olympus).

Immunohistochemical analysis of tumor vascular density

The fresh tumor tissue was sectioned with a cryostat. The tissue thickness was 5 μm, and the tissue sections were adhered to the slide glass and were washed with precooled PBS for twice. The tumor sections were fixed with precooled acetone, fixed at 4°C for 20–30 mins and washed with PBS for 3 times. Each tumor tissue was blocked with goat serum for 30 mins. And tumor tissue was stained and incubated CD31 antibody (1:100) overnight at 4°C in a wet box. Following wash with PBS, goat anti-rabbit HRP-labeled secondary antibody was added and incubated at 37°C for 1 hr. Then, DAB solution was added for color rendering and hematoxylin was used for nuclei staining in each tissue section. The stained sections were observed under a light microscope (Olympus).

Statistical analysis

The data were analyzed by SPSS 15 statistical software (Chicago, IL, USA). The experimental results were expressed as average plus minus SD. The measurement data were analyzed by ANOVA (Tukey test). When $P<0.05$, the statistical difference was significant.

Results

Preparation and characterization of luteolin/Fa-PEG-PCL particles

Luteolin/Fa-PEG-PCL particles were prepared with self-assembly methods (Figure 1). Since Fa-PEG-PCL two block copolymers have amphiphilic molecular properties, because of its surface tension in aqueous solution, the hydrophilic Fa-PEG would diffuse into a shell of spherical particles, and the hydrophobic PCL would cohere and enwrap the same hydrophobic target drug luteolin to form the “nucleus” of the spherical particles. As drug delivery carriers, MPEG-PCL particles have "core shell structure". Because the shell which is formed by MPEG is hydrophilic, luteolin/Fa-PEG-PCL particles can increase the water solubility of luteolin. The process was simulated

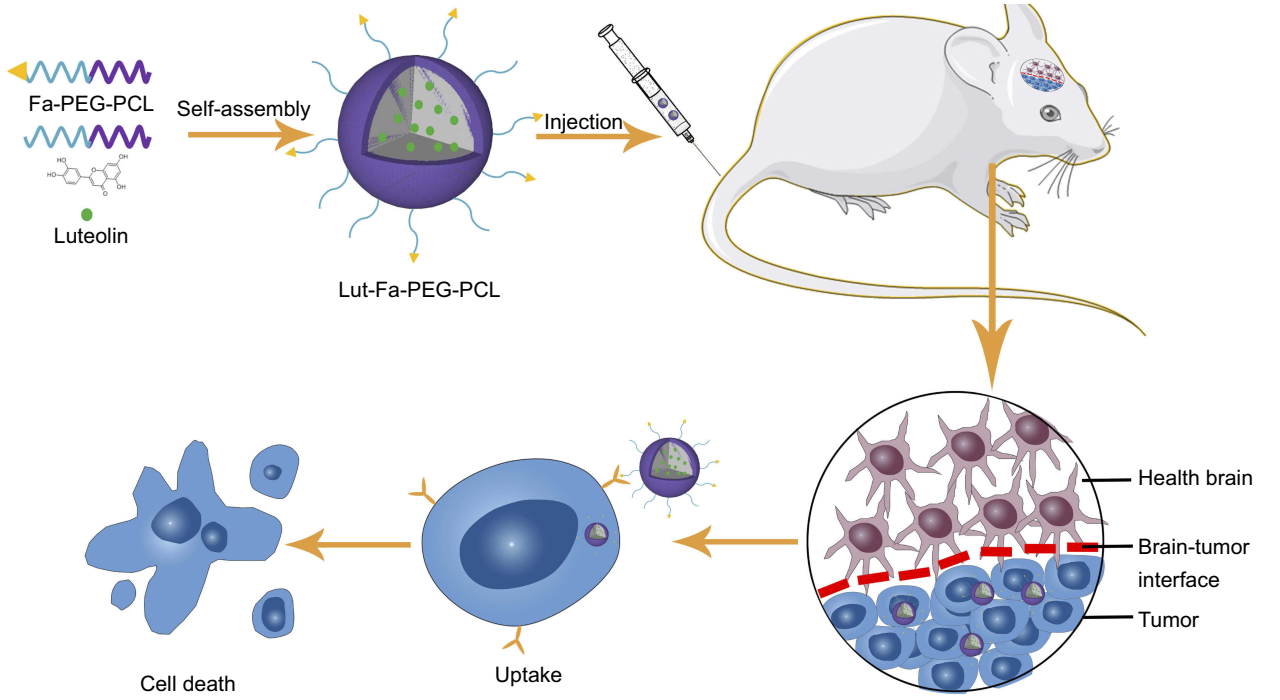

Figure 1 A schematic of the use of Fa-PEG-PCL micelles for antitumor luteolin delivery is illustrated. The first two illustrations demonstrate the synthesis of Lut/Fa-PEG-PCL micelles, which internally encapsulate hydrophobic luteolin with a hydrophilic PEG surface. The latter showed that lut/Fa-PEG-PCL micelles exert antitumor efficacy in the mice in situ glioma model by tail vein injection.
Abbreviations: Lut: luteolin; Fa, folic acid; PEG,polyethylene glycol; PCL, poly-ε-caprolactone.

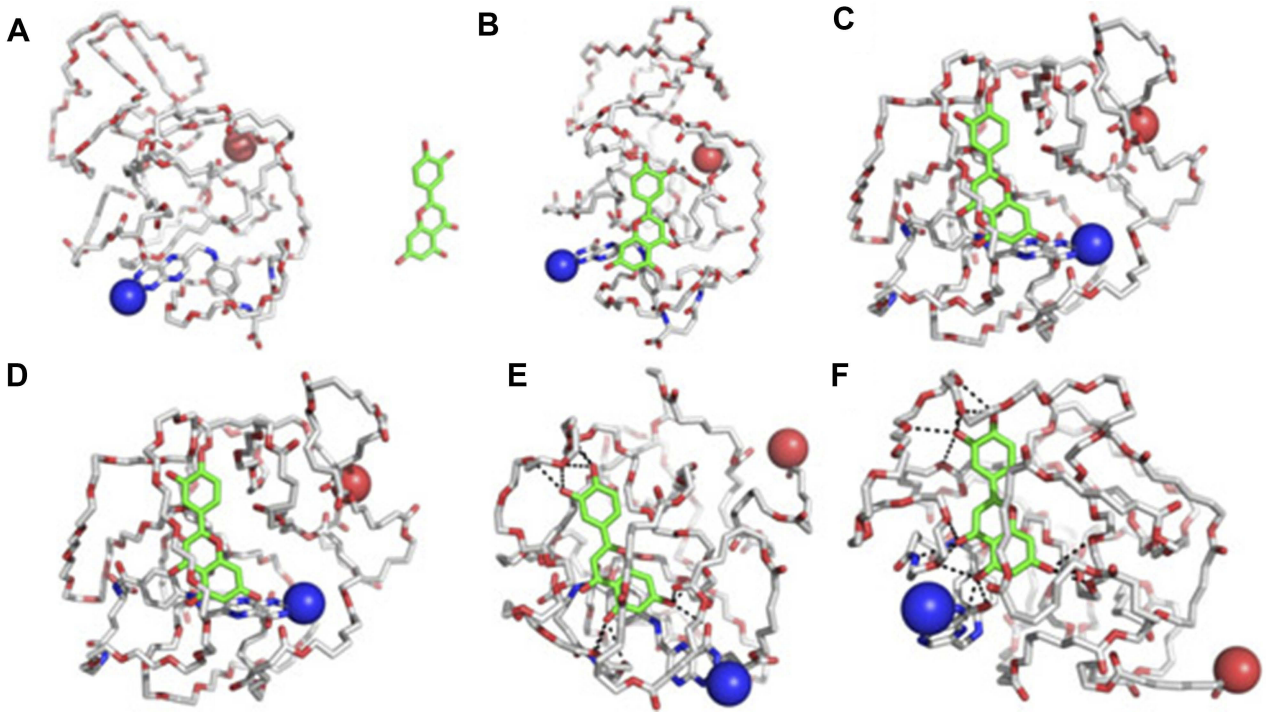

Figure 2 The interaction mode of luteolin and Fa-PEG-PCL copolymer in the water environment. (**A**) Initial structure of a complex composed of luteolin and Fa-PEG-PCL copolymer; conformations (**B**–**F**), respectively, represent 50 ps, 100 ps. Images of composites captured at 200 ps, 300 ps and 400 ps. The Fa-PEG-PCL copolymer is depicted by a thin rod. Luteolin is represented by a thick bar with green carbon atoms. The spherical structure represents the two terminal heavy atoms of the Fa-PEG-PCL copolymer.

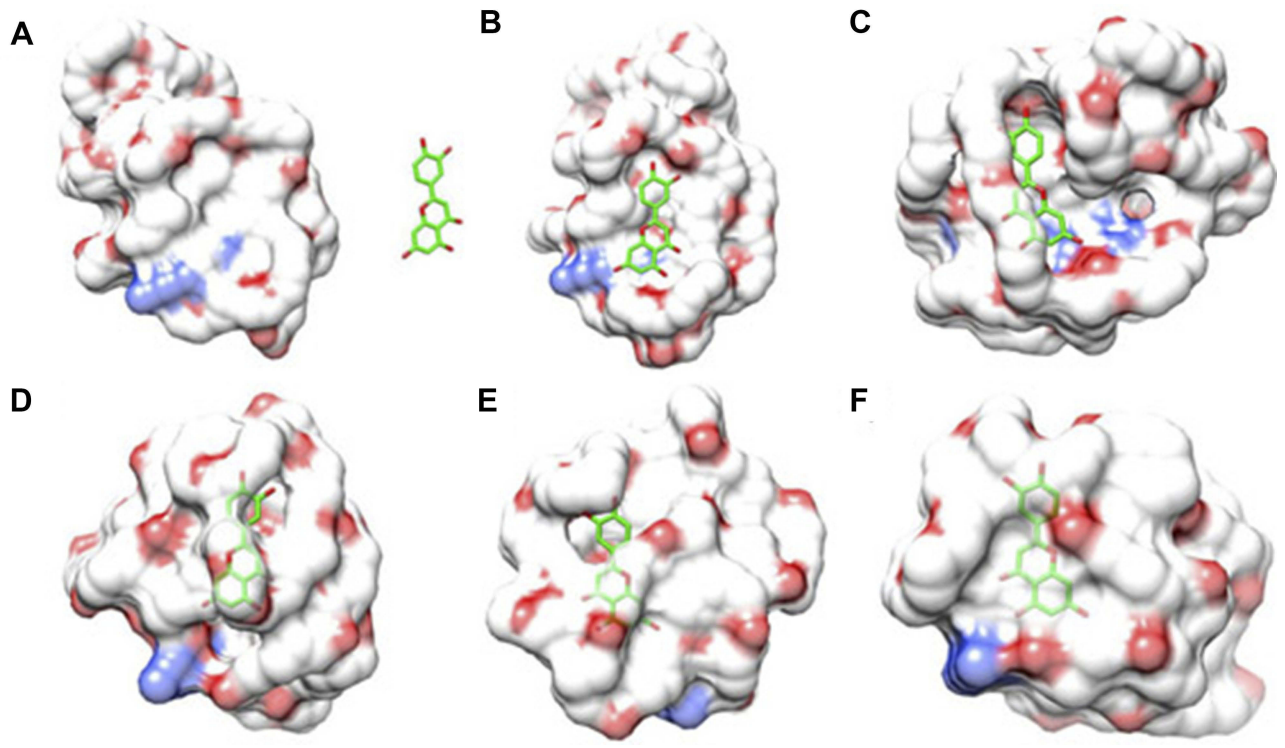

Figure 3 Another mode of interaction between luteolin and Fa-PEG-PCL copolymer in water environment. (**A**) The initial structure of a complex composed of luteolin and Fa-PEG-PCL copolymer; conformations (**B**–**F**), respectively represent 50 ps, 100 ps. Images of composites captured at 200 ps, 300 ps and 400 ps.

by a computer (Figures 2 and 3), which showed that luteolin had a good affinity with Fa-PEG-PCL.

Since folic acid receptors express on the surface of tumors, we modified the edge of PEG with folic acid, so that luteolin nanodrugs can have targeted function. The content of luteolin in the microparticles was determined by HPLC. The DL and ER of luteolin/Fa-PEG-PCL microparticles were calculated, respectively, by formula (1) and formula (2).

The DL was 5% and the ER was 98.5%. The nanoparticle size analyzer measured the luteolin/Fa-PEG-PCL particle size to be 34.7 nm and had a polydispersity index (PDI) of 0.12 (Figure 4). The surface of luteolin/Fa-PEG-PCL particles has a slight negative charge whose zeta potential is −9.2 mv. The results of transmission electron microscopy confirmed the results above. The microscopic particles have a regular spherical structure with a diameter between 25 nm and 30 nm (Figure 4). Since the luteolin/Fa-PEG-PCL particles are relatively loose in the aqueous solution, the nanoparticle size analyzer generally measures the size of the particles to be larger than the transmission electron microscope.

From Figure 5A, free luteolin showed rapid release characteristics and reached the peak 12 hrs later (79.2 ±1.9%), while luteolin/MPEG-PCL particles released only 46% in the initial 10 hrs (another 34%). The luteolin continued to release stably in 70 hrs, implying that luteolin/MPEG-PCL microparticles are stable and sustained releasing of targeted drugs in vitro.

Figure 5B demonstrates different drug concentration–time curves of free luteolin, and luteolin/MPEG-PCL microparticles suggest different pharmacokinetic characteristics. After intravenous injection of the drug in rats, the peaking time (T_{max}) of the free luteolin group (F-Lut) was 15 mins, the half-life of drug elimination ($T_{1/2}$) was 0.63 hrs and the peaking concentration (C_{max}) was 26.32 μg/mL. Area under the curve (area under the curve, AUC) was 15.76; while the luteolin/MPEG-PCL particle group (Lut-M) had a peaking time (T_{max}) of 15 mins, a drug elimination half-life ($T_{1/2}$) of 0.87 hrs and a peaking concentration (C_{max}) of 63.27 μg/mL, with an AUC was 105.7. And the luteolin/Fa-PEG-PCL particle group (Fa-Lut) had a peaking time (T_{max}) of 15 mins, a drug elimination half-life ($T_{1/2}$) of 0.89 hrs and a peaking concentration (C_{max}) of 64.27 μg/mL, with an AUC was 111.7.The peaking time was the same in three groups, but the three factors of the half-life of drug

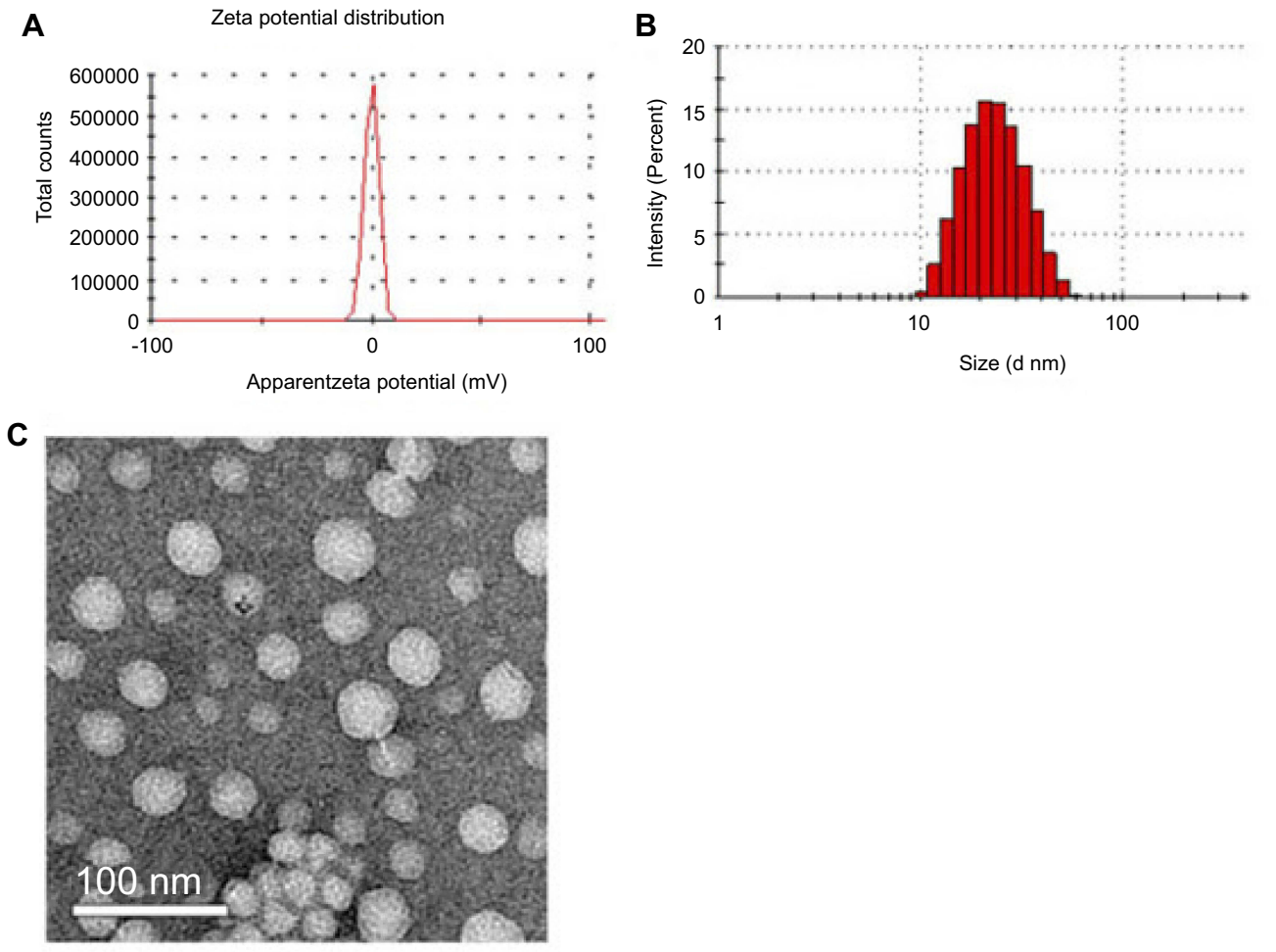

Figure 4 Characterization of Lut/Fa-PEG-PCL micelles. (**A**) Apparent zeta potential of Lut/Fa-PEG-PCL; (**B**) particle size distribution of Lut/Fa-PEG-PCL micelles; (**C**) TEM image of Lut/Fa-PEG-PCL micelles.

elimination ($T_{1/2}$) ($P<0.05$), peak concentration (C_{max}) ($P<0.01$) and AUC ($P<0.01$) were statistically significant.

Experimental results of antiglioma effect in vitro

The results of MTT detection on cell's activity

As shown in Figure 6, free luteolin (F-Lut), luteolin/MPEG-PCL (Lut-M) and luteolin/Fa-PEG-PCL (Fa-Lut) have an effect of inhibiting cellular activity on GL261 glioma cell line and demonstrate an explicit time-dependent and concentration-dependent relationship. As the concentration of luteolin increased from 0.4 μg/mL to 25 μg/mL, the relative cellular viability of GL261 cell line decreased from 94% to 23% at 24 hrs and from 98% at 48 hrs, the decrease was 8%. At the same time, the half-maximal inhibitory concentration (IC_{50}) of free luteolin, luteolin/MPEG-PCL and luteolin/Fa-PEG-PCL against GL261 glioma cell line at 24 hrs was 10.5 μg/mL, 5.5 μg/mL and 3.9 μg/mL, respectively. The results suggested that luteolin/Fa-PEG-PCL nanoparticles were more efficient in killing glioma cells than free luteolin and luteolin/MPEG-PCL. Luteolin's cytotoxicity is enhanced by Fa-PEG-PCL packaging.

The results of the flow cytometry for apoptosis

Inducing apoptosis is the key mechanism for antitumor therapy. In this study, annexin V-fluorescein isothiocyanate (annexin V-FITC) and propidium iodium (PI) apoptosis detection kit were used to detect the situation of free luteolin (F-Lut), luteolin/MPEG-PCL (Lut-M) and luteolin/Fa-PEG-PCL (Fa-Lut) inducing apoptosis of GL261 glioma cells, as shown in Figure 7. The results showed that in the two control groups of normal saline (NS) and blank microparticles (EM), the incidence of apoptosis in GL261 glioma cells was 5.5% and 1.67%, but in the three

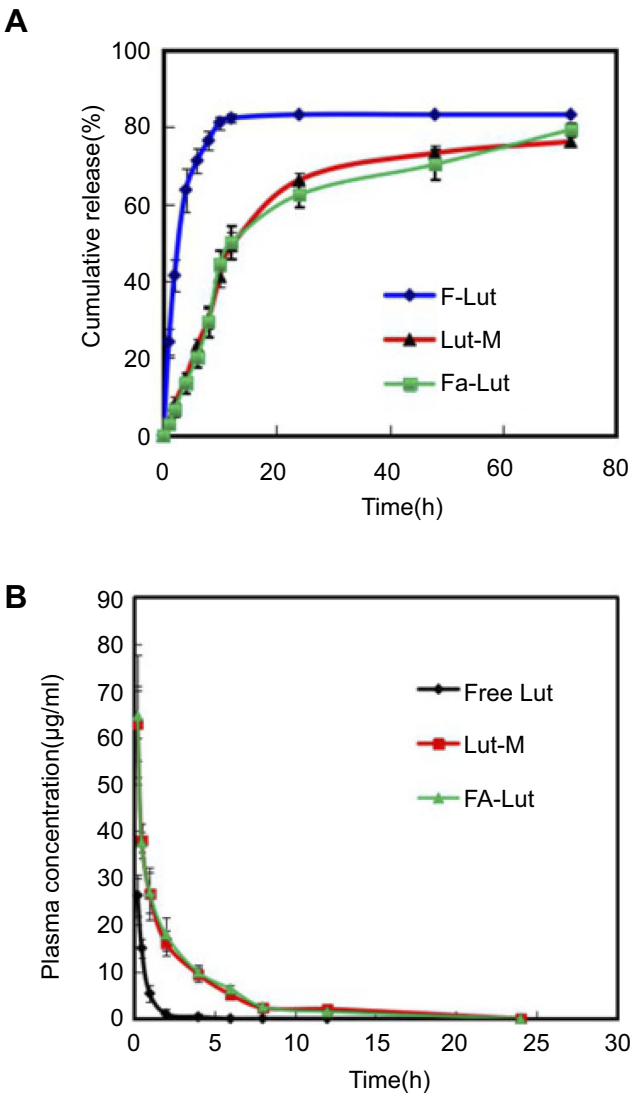

Figure 5 Drug release and pharmacokinetics. (**A**) In vitro drug release; (**B**) in vivo pharmacokinetics of free luteolin (F-Lut), Lut/MPEG-PCL (Lut-M) micelles and Lut/Fa-PEG-PCL (Fa-Lut).

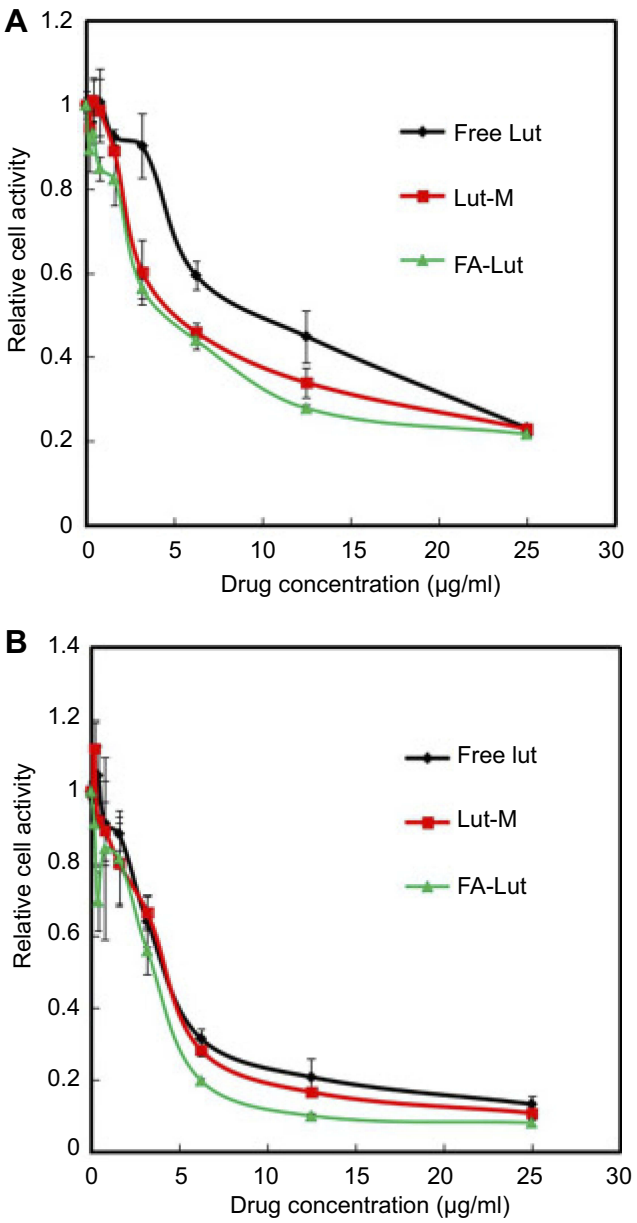

Figure 6 The cytotoxicity of free luteolin, Lut/MPEG-PCL micelles and Lut/Fa-PEG-PCL was investigated by CCK-8 assay. GL261 cells were treated with free luteolin, Lut/MPEG-PCL micelles and Lut/Fa-PEG-PCL at different levels of concentrations for 24 hrs (**A**) and 48 hrs (**B**).

experimental groups of free luteolin (F-Lut), luteolin/MPEG-PCL (Lut-M) and luteolin/Fa-PEG-PCL (Fa-Lut), as shown in Figure 7, the incidence of apoptosis in GL261 glioma cells showed a significant concentration-dependent relationship. In the same 3.125 μg/mL, 6.25 μg/mL and 12.5 μg/mL gradient concentrations, the incidence of apoptosis in GL261 glioma cells of the free luteolin (F-Lut) group, luteolin/MPEG-PCL (Lut-M) group and luteolin/Fa-PEG-PCL (Fa-Lut) group was 8.51%, 3.43% and 7.19%, 16.33%, 23.36% and 41.02%, 41.3%, 50.65% and 69.3%, respectively. The results above showed that luteolin/Fa-PEG-PCL was more powerful in apoptosis inducing of GL261 glioma cells than free luteolin and luteolin/MPEG-PCL ($P<0.05$).

Experimental results of antiglioma effect in vivo

In the mice subcutaneous model of GL261, luteolin showed significant antitumor effect and had no significant effect on mouses' weight. The relevant experimental data and the subcutaneous glioma of tumor-bearing mice were photographed during the experiment and are shown in Figures 8 and 9. Figure 8 shows that free luteolin, luteolin/MPEG-PCL and luteolin/Fa-PEG-PCL nanoparticles have strong antitumor effects on GL261 glioma cells, with tumors

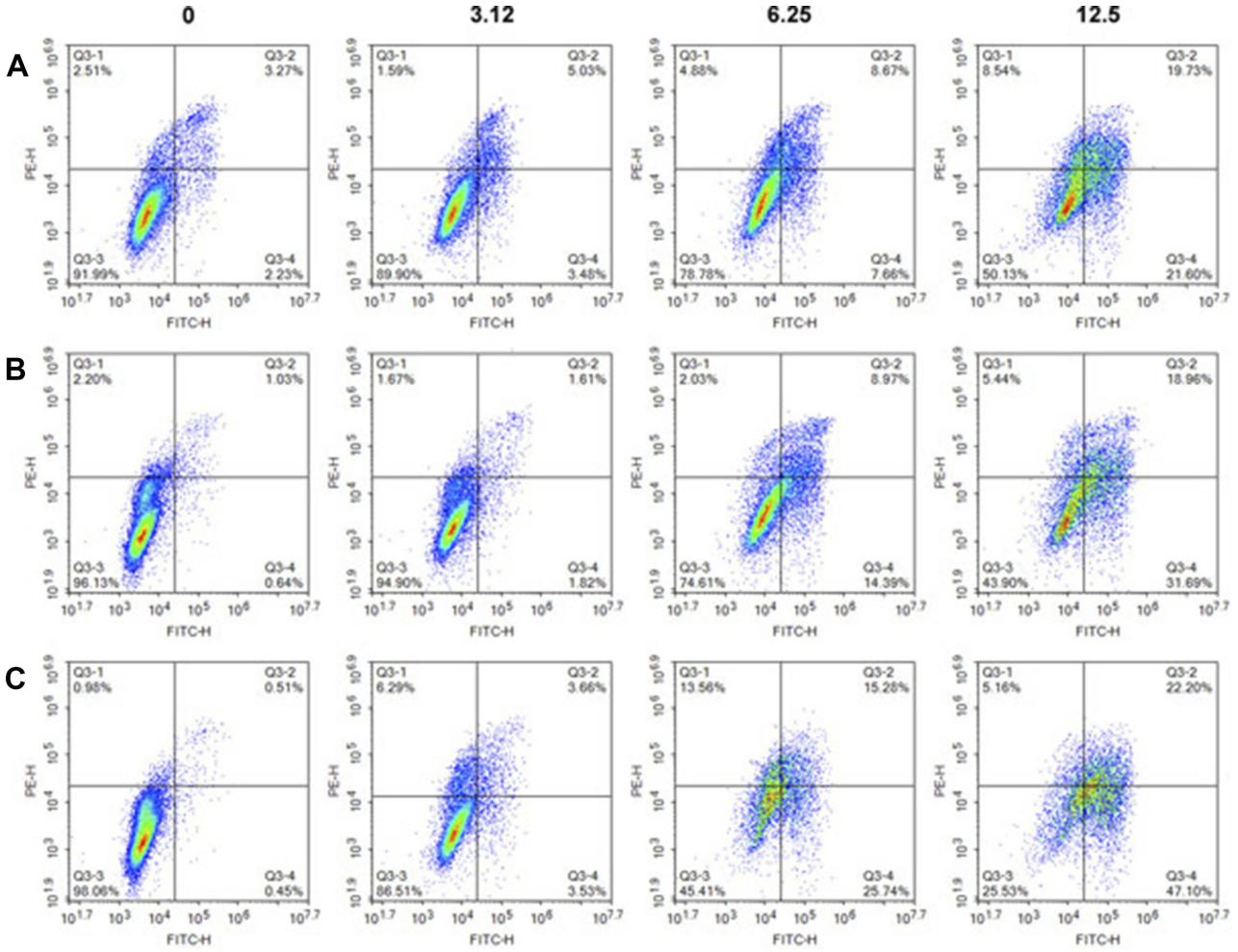

Figure 7 Apoptosis studies were performed using FCM. GL261 cells were cultured in 6-well plates for 24 hrs and then incubated with luteolin (**A**) lut/MPEG-PCL micelles (**B**) and lut/Fa-PEG-PCL (**C**) at different level of lut concentrations for 48 hrs.

shrinking by 52% (F-Lut), 67% (Lut-M) and 81% (Fa-Lut), respectively. Comparing the luteolin/Fa-PEG-PCL drug-carried nanoparticle experimental group with other groups, its antitumor effect was significantly stronger than other groups ($P<0.01$). And the experimental results in the animal models of subcutaneous and intracranial orthotopic tumor were consistent. Figure 9 shows that free luteolin, luteolin/MPEG-PCL and luteolin/Fa-PEG-PCL have strong antitumor effects in intracranial orthotopic model. At the same time, Figure 8 shows that the tumor weight of the luteolin/Fa-PEG-PCL nanoparticle experimental group was significantly lower than that of the other groups ($P<0.01$), further suggesting that Fa-PEG-PCL enhances the antitumor effect, becoming an ideal delivery carrier.

In addition, there was no significant change in the weight of mouse during the antitumor experiment, suggesting that the cytotoxicity of the luteolin/Fa-PEG-PCL nanoparticles is not obvious.

Effects of luteolin/Fa-PEG-PCL on proliferation antiangiogenesis and apoptosis in vivo

The expression of CD31 is often used to assess tumor angiogenesis. As shown in Figure 10, the expression of CD31 was higher in the saline group (NS) and the blank particle group (EM), suggesting that the number of microvessels was higher in neonatal tumor. And in the the free luteolin group (F-Lut), luteolin/MPEG-PCL nanoparticle group (Lut-M) and luteolin/Fa-PEG-PCL nanoparticle group (Fa-Lut), the number of microvessels in the neonatal tumor was significantly reduced to 17.3±5.2, 11.3±3.1 and 4.1±2.2, respectively. The number of microvessels in tumor was 37.8±7.3 in the saline group (NS) and 33.4±7.2 in the blank microparticle group (EM), which were significantly higher than luteolin/Fa-PEG-PCL drug-carried nanoparticle group ($P<0.01$), suggesting that luteolin/FaPEG-PCL

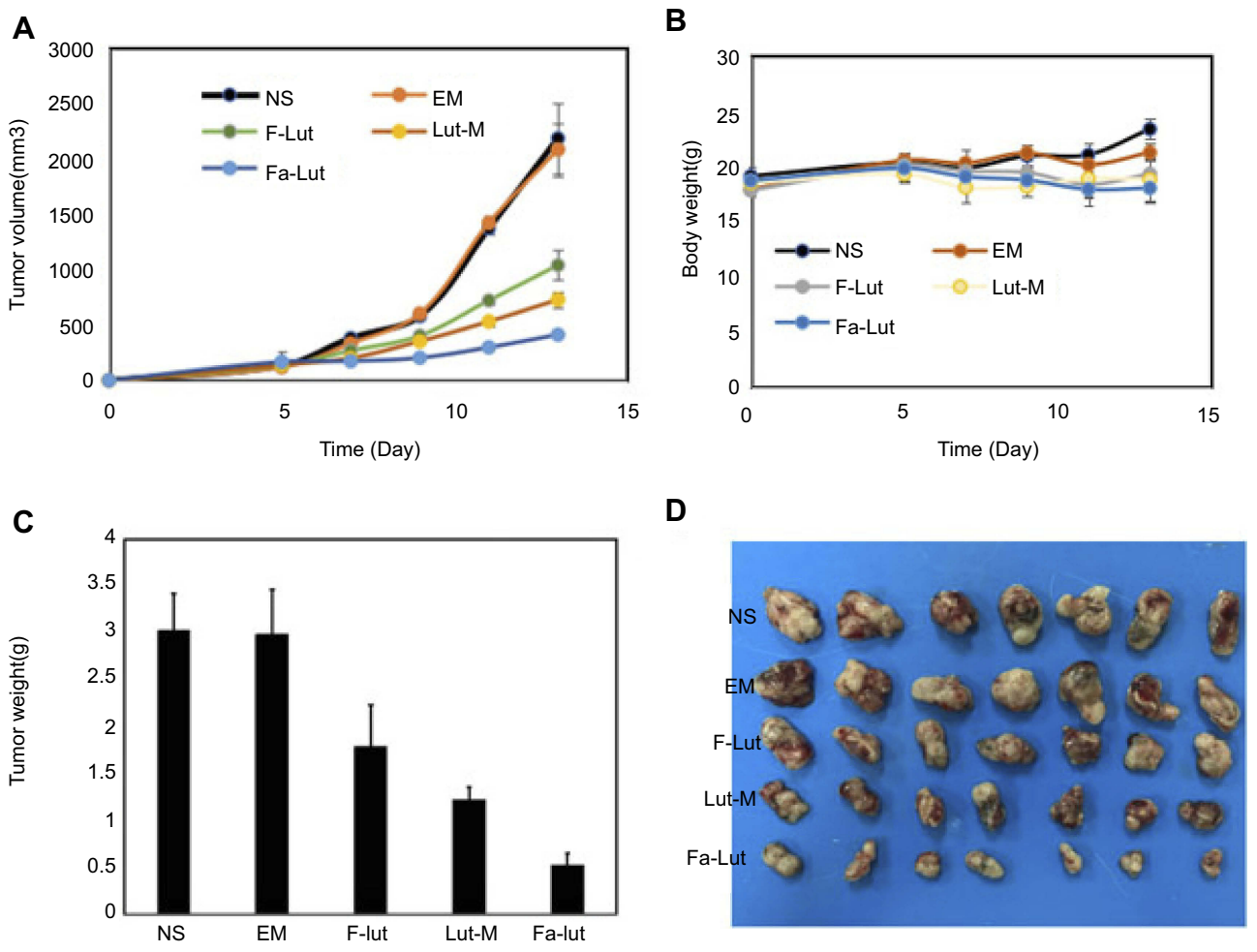

Figure 8 Female C57 mice were injected with GL261 cells to generate a subcutaneous xenograft tumor model. When the tumor volume reached 0.1 cm^3, they were randomly divided into 5 groups and received treatment with NS, EM, F-Lut, Lut-M and Fa-Lut, respectively. (**A**) Five groups of body weights were measured every other day; (**B**) Tumor growth curve; (**C**) tumor weight measured in different groups; (**D**) representative tumor photographs in each treatment group on day 13.

nanoparticles could significantly inhibit the neovascularization of GL261 glioma, which may play an important role in inhibiting tumor cellular growth.

PCNA is an important marker for detecting cell proliferation activity. In this study, the expression of PCNA was detected by immunohistochemical to understand the cell proliferation activity of GL261 glioma cells in the subcutaneous tumor model of nude mice. As shown in Figure 11, a large amount of red fluorescence emitted by PCNA-staining-positive cells was observed in the saline group (NS), the blank particle group (EM), and the free luteolin group (F-Lut), while in the group of luteolin/MPEG-PCL drug-carried nanoparticle group (Lut-M), the PCNA-staining-positive cells were significantly reduced. The PCNA proliferation index was the lowest in the luteolin/Fa-PEG-PCL drug-carried nanoparticle group (Fa-Lut), which was only 12.2±3.15%, while in the saline group (NS), it was as high as 78.3±7.2% in the blank particles, 79.3±7.2% in the blank particle group (EM), 63.2±5.3% in the group of free luteolin (F-Lut) and reached 33.2±7.9% in the group of luteolin/MPEG-PCL (Lut-M). The proliferation index of PCNA cells was significantly lower in the luteolin/Fa-PEG-PCL drug-carried nanoparticle group than in other groups ($P<0.01$), suggesting that luteolin/Fa-PEG-PCL drug-carried nanoparticles can inhibit the ability of GL261 glioma cells to proliferate significantly.

The results of the TUNEL method for detecting apoptosis of GL261 glioma cells in vivo are shown in Figure 12. As shown in Figure 10, we did not find TUNEL-positive apoptotic cells in the control group of the saline group (NS) or the blank particle group (EM). But a large number of tumor cells positive for TUNEL staining were found in the

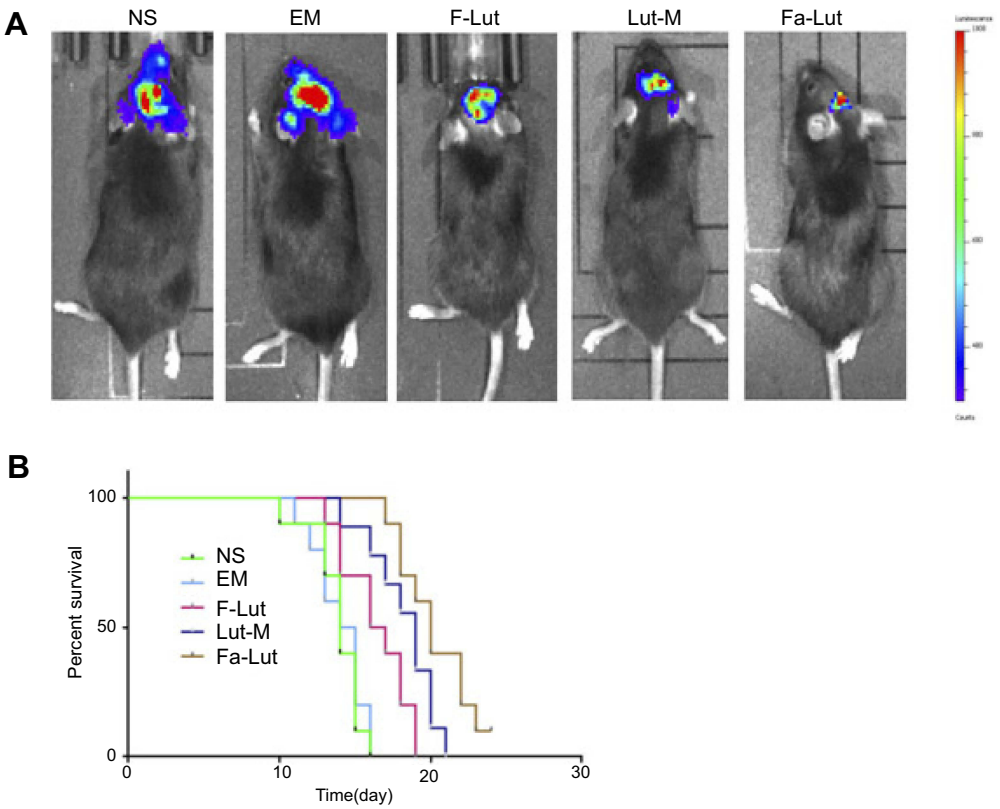

Figure 9 Bioimaging analysis of the GL261 in situ mouse model. (**A**) Intracerebral gliomas were observed by using fluorescent markers. Fa-Lut is more effective in inhibiting tumors than other groups. (**B**) Life survival time assessment. F-lut, lut-M and Fa-lut prolonged the lifespan of mice, while mice in the Fa-lut group survived longer.

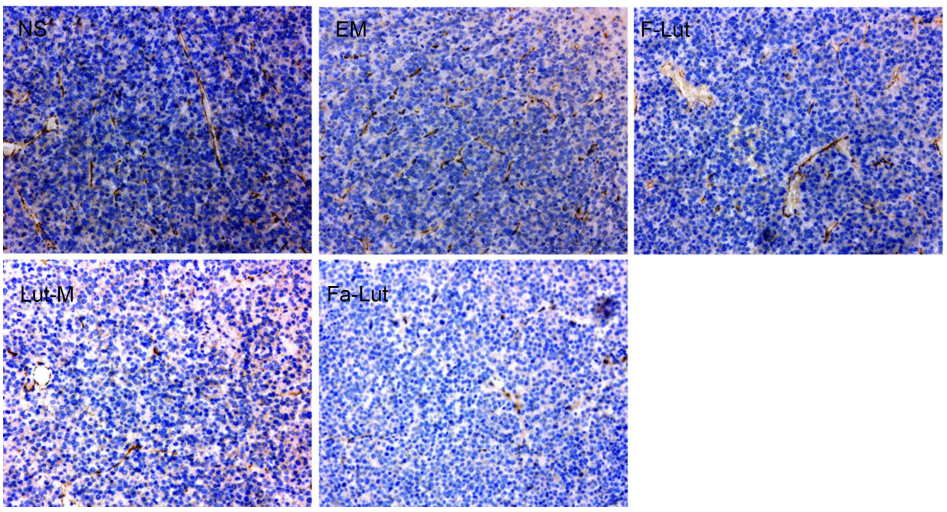

Figure 10 Immunohistochemical analysis of CD31. CD31, a marker of angiogenesis, was detected by immunohistochemistry in tumor tissues treated with NS, EM, F-Lut, Lut-M and Fa-Lut.

F-Lut and Lut-M and Fa-Lut groups. The apoptotic indexes of each group were shown as follows: saline group (NS) was 4.3±1.7%, blank particle group (EM) was 3.5±1.35% and free luteolin group (F-Lut) was 21.0±4.4%. The group of luteolin/MPEG-PCL drug-carried nanoparticle (Lut-M) was 37.0±7.3%. The group of luteolin/Fa-PEG-PCL drug-

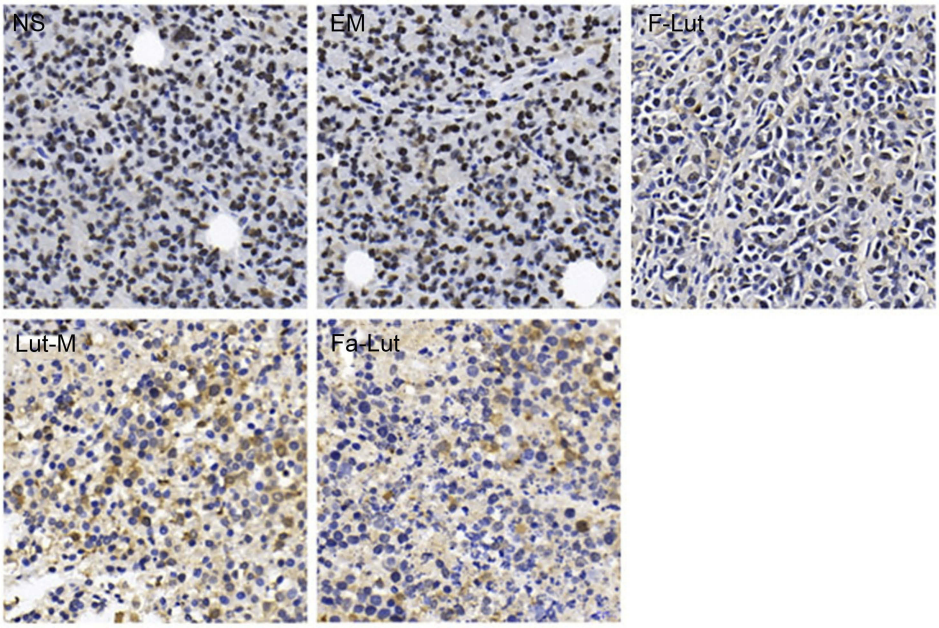

Figure 11 Immunohistochemical analysis of PCNA. Mechanism of antitumor effect of Fa-lut micelles on GL261 subcutaneous mouse model. PCNA antibody was used to stain tumor sections of five groups, in order to evaluate the proliferation of tumor cell.

carried nanoparticle (Fa-Lut) was 61.0±11.2%. The luteolin/Fa-PEG-PCL nanoparticle group showed more obvious apoptosis than other groups (P<0.01), suggesting that luteolin can significantly enhance the ability of inducing apoptosis of GL261 glioma cells in vivo through being coated by Fa-PEG-PCL into nanoparticles.

Safety assessment

Safety assessment of luteolin was also performed according to body weight changes and histological analysis of vital organs. As shown in Figure 8B, there were no significant changes in body weights from each group in subcutaneous tumor models (p>0.05). In addition, the H&E staining of heart, liver, lung, kidney and spleen showed no obvious histopathological abnormalities, lesions, degenerations or necrosis in each group (Figure 13).

Discussion

Luteolin has a broad-spectrum antitumor effect, which can directly inhibit the proliferation of tumor cells, antagonize the carcinogenic effects of carcinogens and induce apoptosis by regulating cell cycle and activating endogenous and exogenous pathways.[25,26] Luteolin also has antitumor effects of invasion and metastasis, antitumor angiogenesis and chemotherapy sensitization effects.[27,28] The antitumor effect of luteolin involved complex signal transduction pathways and regulatory mechanisms. It was found that luteolin had many different kinds of antitumor effects through a variety of in

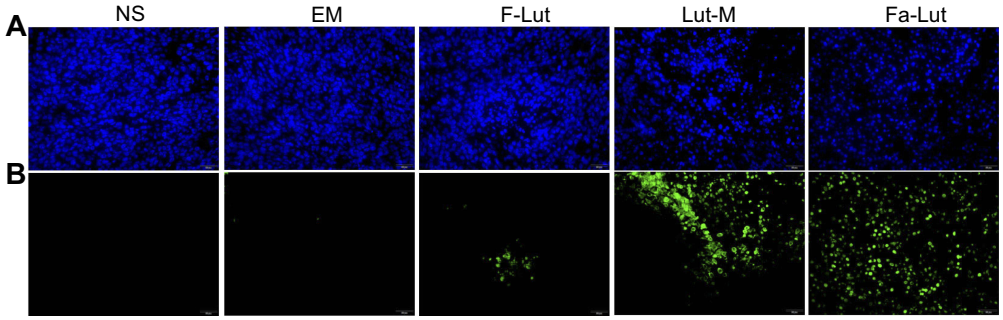

Figure 12 TUNNEL assay. Tumor cell apoptosis was studied by TUNNEL staining. (**A**) DAPI staining; (**B**) Tunnel staining. Comparing to the other groups, Fa-lut promoted more apoptosis in GL261 cells. Five groups of tumor tissues were all stained with DAPI.

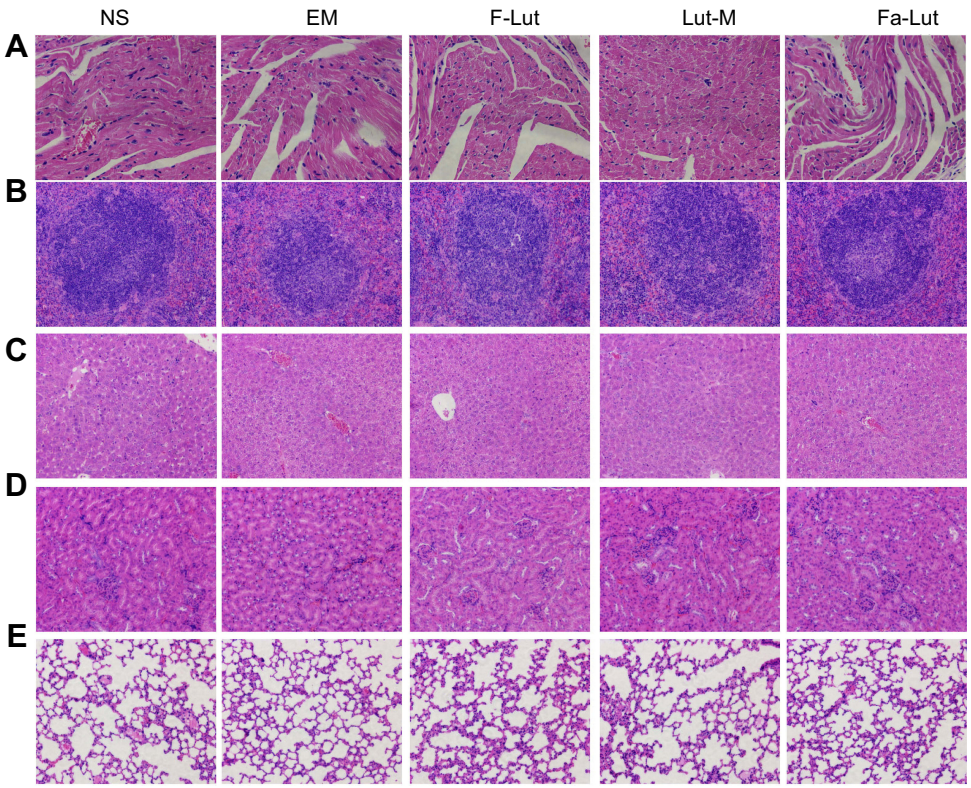

Figure 13 In vivo toxicity assessment and histological images. The vital organs (heart (**A**), spleen (**B**), liver (**C**), kidney (**D**) and lung (**E**)) were collected from the mice and histologically examined under a microscope using HE staining. All groups showed normal histomorphology.

vitro and in vivo antiglioma experiments. Oral luteolin is not recommended because of its low absorption rate and first-pass effect, and its bioavailability is not ideal. Thus, taking luteolin is generally not recommended. Studies have shown that the oral absorption rate of rats fed with high dose of 100 mg/kg luteolin is only 10%, and the maximum plasma concentration is only 3.79 μg/mL, and due to the rapid clearance of luteolin in plasma, both oral and intravenous injections are difficult to achieve effective plasma concentrations.[29] Drug delivery via MPEG-PCL nanoparticles is expected to solve this problem.

An important reason for the current poor efficacy and poor prognosis of GBM is the inefficiency of chemotherapy drugs. Due to the presence of a special BBB in the central nervous system, most chemotherapy drugs are difficult to reach brain parenchyma cells or tumor cells through BBB.[30–32] Even if the drug passes through the BBB, it is difficult to achieve drug concentration inhibition or killing of tumor cells. The folate-modified luteolin/MPEG-PCL drug-carried nanoparticles prepared in this study averaged 34.7 nm in diameter, while the intercellular junctions of tumor cells were generally 40 nm to 80 nm, so folic acid-modified luteolin/Fa-PEG -PCL nanoparticles can pass through this barrier more easily by active diffusion. At the same time, because MPEG-PCL drug-carried nanoparticles have the characteristics of gradually degrading and releasing drugs in the body, it helps the target drug to reach the concentration required for treatment and maintains its therapeutic effect.

In the meanwhile, luteolin can also effectively improve its physical and chemical properties after being formed into nanoparticles by MPEG-PCL packaging. The MPEG-PCL diblock copolymer with amphiphilic properties forms a unique "shell-core structure" in aqueous solution due to surface tension. The hydrophilic MPEG will diffuse to form the "shell" of the spherical particle appearance and the hydrophobic PCL will envelope the same hydrophobic drug luteolin to form the "nucleus" of the spherical particles. Since the “shell” formed by MPEG is hydrophilic, luteolin can also increase the water solubility of luteolin after being packaged by MPEG-PCL. At the same time, MPEG nanoparticles have the effect of preventing protein adsorption during blood circulation from being removed, and the “shell-core structure” has a slow-release effect; therefore, it can maintain a high drug concentration.[33–35]

The in vitro release characteristics and in vivo pharmacokinetics of luteolin after folic acid-modified MPEG-PCL packaging showed significant changes. Compared with free luteolin, folic acid-modified luteolin nanoparticles and luteolin nanoparticles perform stable, long-lasting vitro release characteristics, along with longer half-lives, higher peak concentrations and larger area under the curves, which indicates that folic acid-modified luteolin/MPEG-PCL and packed MPEG-PCL form into nanoparticles, which greatly improves the bioavailability and pharmacokinetic characteristics of luteolin and achieves the ideal delivery effect of long-lasting drug release and long-lasting effect. It is because of the pharmacokinetic characteristics above that luteolin nanoparticles exhibit a stronger antiglioma effect in vivo and in vitro. In addition, targeted therapy provides a good platform for the treatment of tumors. In this study, folic acid was used to modify PEG-PCL and could recognized the folate receptor which is expressed on the surface of the tumor to achieve the targeted therapy.

The results of in vitro MTT assay showed that (Figure 3) free luteolin, luteolin nanoparticles and folic acid-modified nanodrugs inhibited cell viability in GL261 glioma cells, showing significant time dependence and concentration dependence. Fotsis et al reported that luteolin has the strongest inhibiting cell proliferation on normal human cells such as breast cancer cell line MCF-7 and other tumor cell lines,[36,37] which is similar to the results of this study. Moreover, after the luteolin was encapsulated by the nanopreparation, the antitumor effect was increased. After being modified by folic acid, the curative effect of luteolin nanoparticles was further improved. It indicates that folic acid-modified luteolin nanoparticles have stronger antitumor cell proliferation compared with free drugs and nanodrugs.

In the in vivo model of subcutaneous tumors and intracranial tumors in GL261 glioma mice, free luteolin, luteolin nanoparticles and folic acid-modified nanodrugs all showed antitumor effect. Glioma was inhibited by 42.7%, 59.5% and 81.2%, respectively. In the intracranial tumor model, it was found that the lifespan of the treated mice was significantly prolonged, and the treatment of folic acid modification was the best. Fang et al studied the antitumor effect of luteolin on the heterologous inhibition model of prostate tumor PC-3 nude mice and found that after 18 days, the tumor weight was 180 mg in the control group without luteolin intervention. The tumor weight of the 5 mg/kg luteolin intraperitoneal injection group was 125 mg, and the tumor weight of the 10 mg luteolin injection group was 110 mg. There was a statistical difference between the intervention group and the control group (P=0.011), which was consistent with the results of this study.

Tumor neovascularization is inseparable of tumor growth, infiltration and metastasis.[38–40] In this study, the effect of luteolin on tumor angiogenesis was evaluated by detecting the expression of CD31. It was found that in the two control groups of saline and blank microparticles, the number of neovascular microvessels was 67.8 and 66.4, respectively, while in the three experimental groups of free luteolin, luteolin nanometers and folic acid-modified nanomedicine, the number of microvessels in neonatal tumors was significantly reduced, which were 45.2, 27 and 12.0, respectively, which suggests that luteolin has an important role in inhibiting tumor angiogenesis. Studies have shown that luteolin performs strong antitumor angiogenesis in chicken chorioallantoic membrane; this study found that luteolin also inhibits tumor angiogenesis in GL261 glioma, and the results are consistent with the study mentioned above. In addition, luteolin induces tumor cell apoptosis and inhibits tumor cell proliferation in vivo, effectively inhibiting tumor growth, and folic acid-modified luteolin nano-drugs have the best inhibitory effect. In addition, this study found that there was no significant change in body weight of mice during experiments in vivo, which suggests that the cytotoxicity of free luteolin, luteolin/MPEG-PCL drug-loaded nanoparticles and folic acid-modified nanodrugs is not obvious, and all have high biosafety.

In summary, folic acid-modified PEG-PCL nanoparticles were used for the delivery of luteolin, improving the pharmacokinetic characteristics and sustaining the drug release of luteolin. Luteolin/Fa-PEG-PCL significantly enhanced the antiglioma effect through inducing more cell apoptosis, inhibiting more cell proliferation and suppressing more neovascularization of glioma. Luteolin/Fa-PEG-PCL may be a new drug to treat glioma in the future.

Acknowledgment

This work was financially supported by Sichuan Science and Technology Project (No.2018FZ0028).

Disclosure

The authors report no conflict of interest in this study.

References

1. Alcantara Llaguno SR, Wang Z, Sun D, et al. Adult lineage-restricted CNS progenitors specify distinct glioblastoma subtypes. *Cancer Cell*. 2015;28(4):429–440. doi:10.1016/j.ccell.2015.09.007

2. Zhao HF, Wang J, Shao W, et al. Recent advances in the use of PI3K inhibitors for glioblastoma multiforme: current preclinical and clinical development. *Mol Cancer*. 2017;16(1):100. doi:10.1186/s12943-017-0670-3
3. Thomas AA, Brennan CW, DeAngelis LM, Omuro AM. Emerging therapies for glioblastoma. *JAMA Neurol*. 2014;71(11):1437–1444. doi:10.1001/jamaneurol.2014.1701
4. Wang F, Wang AY, Chesnelong C, et al. ING5 activity in self-renewal of glioblastoma stem cells via calcium and follicle stimulating hormone pathways. *Oncogene*. 2018;37(3):286–301.
5. Tian R, Wang J, Yan H, et al. Differential expression of miR16 in glioblastoma and glioblastoma stem cells: their correlation with proliferation, differentiation, metastasis and prognosis. *Oncogene*. 2017;36(42):5861–5873.
6. Zhong JD, Feng Y, Li HM, Xia XS, Li RT. A new flavonoid glycoside from Elsholtzia bodinieri. *Nat Prod Res*. 2016;30(20):2278–2284.
7. Al-Qudah MA, Otoom NK, Al-Jaber HI, et al. New flavonol glycoside from Scabiosa prolifera L. aerial parts with in vitro antioxidant and cytotoxic activities. *Nat Prod Res*. 2017;31(24):2865–2874.
8. He Y, Xia Z, Yu D, et al. Hepatoprotective effects and structure-activity relationship of five flavonoids against lipopolysaccharide/d-galactosamine induced acute liver failure in mice. *Int Immunopharmacol*. 2019;68:171–178.
9. Xiao N, Mei F, Sun Y, Pan G, Liu B, Liu K. Quercetin, luteolin, and epigallocatechin gallate promote glucose disposal in adipocytes with regulation of AMP-activated kinase and/or sirtuin 1 activity. *Planta Med*. 2014;80(12):993–1000.
10. Maatouk M, Mustapha N, Mokdad-Bzeouich I, et al. Thermal treatment of luteolin-7-O-beta-glucoside improves its immunomodulatory and antioxidant potencies. *Cell Stress Chaperones*. 2017;22(6):775–785. doi:10.1007/s12192-017-0808-7
11. Wang L, Li W, Lin M, et al. Luteolin, ellagic acid and punicic acid are natural products that inhibit prostate cancer metastasis. *Carcinogenesis*. 2014;35(10):2321–2330. doi:10.1093/carcin/bgu145
12. Tang L, Li Y, Chen WY, et al. Breast cancer resistance protein-mediated efflux of luteolin glucuronides in HeLa cells overexpressing UDP-glucuronosyltransferase 1A9. *Pharm Res*. 2014;31(4):847–860. doi:10.1007/s11095-013-1207-0
13. Liu H, Zeng Z, Wang S, et al. Main components of pomegranate, ellagic acid and luteolin, inhibit metastasis of ovarian cancer by down-regulating MMP2 and MMP9. *Cancer Biol Ther*. 2017;18(12):990–999. doi:10.1080/15384047.2017.1394542
14. Cook MT, Liang Y, Besch-Williford C, Hyder SM. Luteolin inhibits lung metastasis, cell migration, and viability of triple-negative breast cancer cells. *Breast Cancer*. 2017;9:9–19.
15. Sonoki H, Tanimae A, Endo S, et al. Kaempherol and luteolin decrease claudin-2 expression mediated by inhibition of STAT3 in lung adenocarcinoma A549 cells. *Nutrients*. 2017;9:6. doi:10.3390/nu9060597
16. Kwon EJ, Skalak M, Lo Bu R, Bhatia SN. Neuron-targeted nanoparticle for siRNA delivery to traumatic brain injuries. *ACS Nano*. 2016;10(8):7926–7933. doi:10.1021/acsnano.6b03858
17. Saraiva C, Praca C, Ferreira R, Santos T, Ferreira L, Bernardino L. Nanoparticle-mediated brain drug delivery: overcoming blood-brain barrier to treat neurodegenerative diseases. *J Controlled Release*. 2016;235:34–47. doi:10.1016/j.jconrel.2016.05.044
18. Anraku Y, Kuwahara H, Fukusato Y, et al. Glycaemic control boosts glucosylated nanocarrier crossing the BBB into the brain. *Nat Commun*. 2017;8(1):1001. doi:10.1038/s41467-017-00952-3
19. Aslund AKO, Berg S, Hak S, et al. Nanoparticle delivery to the brain–by focused ultrasound and self-assembled nanoparticle-stabilized microbubbles. *J Controlled Release*. 2015;220(Pt A):287–294. doi:10.1016/j.jconrel.2015.10.047
20. Ye D, Raghnaill MN, Bramini M, et al. Nanoparticle accumulation and transcytosis in brain endothelial cell layers. *Nanoscale*. 2013;5(22):11153–11165. doi:10.1039/c3nr02905k
21. Jones SK, Sarkar A, Feldmann DP, Hoffmann P, Merkel OM. Revisiting the value of competition assays in folate receptor-mediated drug delivery. *Biomaterials*. 2017;138:35–45. doi:10.1016/j.biomaterials.2017.05.034
22. Xu L, Bai Q, Zhang X, Yang H. Folate-mediated chemotherapy and diagnostics: an updated review and outlook. *J Controlled Release*. 2017;252:73–82. doi:10.1016/j.jconrel.2017.02.023
23. Liu X, Wang B, Li Y, et al. Powerful anticolon tumor effect of targeted gene immunotherapy using folate-modified nanoparticle delivery of CCL19 to activate the immune system. *ACS Cent Sci*. 2019;5(2):277–289. doi:10.1021/acscentsci.8b00688
24. Gao X, Wang S, Wang B, et al. Improving the anti-ovarian cancer activity of docetaxel with biodegradable self-assembly micelles through various evaluations. *Biomaterials*. 2015;53:646–658. doi:10.1016/j.biomaterials.2015.02.108
25. Cao Z, Zhang H, Cai X, et al. Luteolin promotes cell apoptosis by inducing autophagy in hepatocellular carcinoma. *Cell Physiol Biochem*. 2017;43(5):1803–1812. doi:10.1159/000484066
26. Wang F, Gao F, Pan S, Zhao S, Xue Y. Luteolin induces apoptosis, G0/G1 cell cycle growth arrest and mitochondrial membrane potential loss in neuroblastoma brain tumor cells. *Drug Res*. 2015;65(2):91–95. doi:10.1055/s-0034-1372648
27. Lee WJ, Wu LF, Chen WK, Wang CJ, Tseng TH. Inhibitory effect of luteolin on hepatocyte growth factor/scatter factor-induced HepG2 cell invasion involving both MAPK/ERKs and PI3K-Akt pathways. *Chem Biol Interact*. 2006;160(2):123–133. doi:10.1016/j.cbi.2006.01.002
28. Lin D, Kuang G, Wan J, et al. Luteolin suppresses the metastasis of triple-negative breast cancer by reversing epithelial-to-mesenchymal transition via downregulation of beta-catenin expression. *Oncol Rep*. 2017;37(2):895–902. doi:10.3892/or.2016.5311
29. Lin LC, Pai YF, Tsai TH. Isolation of luteolin and luteolin-7-O-glucoside from dendranthema morifolium ramat tzvel and their pharmacokinetics in rats. *J Agric Food Chem*. 2015;63(35):7700–7706. doi:10.1021/jf505848z
30. Pardridge WM. CSF, blood-brain barrier, and brain drug delivery. *Expert Opin Drug Deliv*. 2016;13(7):963–975. doi:10.1517/17425247.2016.1171315
31. Patel MM, Patel BM. Crossing the blood-brain barrier: recent advances in drug delivery to the brain. *CNS Drugs*. 2017;31(2):109–133. doi:10.1007/s40263-016-0405-9
32. Alyautdin R, Khalin I, Nafeeza MI, Haron MH, Kuznetsov D. Nanoscale drug delivery systems and the blood-brain barrier. *Int J Nanomedicine*. 2014;9:795–811. doi:10.2147/IJN.S52236
33. Larson TA, Joshi PP, Sokolov K. Preventing protein adsorption and macrophage uptake of gold nanoparticles via a hydrophobic shield. *ACS Nano*. 2012;6(10):9182–9190. doi:10.1021/nn3035155
34. Lin W, Garnett MC, Schacht E, Davis SS, Illum L. Preparation and in vitro characterization of HSA-mPEG nanoparticles. *Int J Pharm*. 1999;189(2):161–170.
35. Lin W, Garnett MC, Davis SS, Schacht E, Ferruti P, Illum L. Preparation and characterisation of rose Bengal-loaded surface-modified albumin nanoparticles. *J Controlled Release*. 2001;71(1):117–126.
36. Sato Y, Sasaki N, Saito M, Endo N, Kugawa F, Ueno A. Luteolin attenuates doxorubicin-induced cytotoxicity to MCF-7 human breast cancer cells. *Biol Pharm Bull*. 2015;38(5):703–709.
37. George VC, Naveen Kumar DR, Suresh PK, Kumar S, Kumar RA. Comparative studies to evaluate relative in vitro potency of luteolin in inducing cell cycle arrest and apoptosis in HaCaT and A375 cells. *Asian Pac J Cancer Prev*. 2013;14(2):631–637.

38. Fang J, Zhou Q, Shi XL, Jiang BH. Luteolin inhibits insulin-like growth factor 1 receptor signaling in prostate cancer cells. *Carcinogenesis*. 2007;28(3):713–723.
39. Kazemi M, Carrer A, Moimas S, et al. VEGF121 and VEGF165 differentially promote vessel maturation and tumor growth in mice and humans. *Cancer Gene Ther*. 2016;23(5):125–132.
40. Swierczak A, Mouchemore KA, Hamilton JA, Anderson RL. Neutrophils: important contributors to tumor progression and metastasis. *Cancer Metastasis Rev*. 2015;34(4):735–751.